OFFICE OF NAVAL RESEARCH

GRANT or CONTRACT: N00014-91J-1201

R&T CODE: 4133032
Richard Carlin

TECHNICAL REPORT NO. 31

"An Electrochemically-Driven Actuator Based on a Nanostructured Carbon Material"

Guangli Che, Scott A. Miller, Ellen R. Fisher, and Charles R. Martin

Prepared for Publication

in

Analytical Chemistry

Colorado State University
Department of Chemistry
Fort Collins, CO 80523-1872

June 1, 1999

REPORT DOCUMENTATION PAGE

1. June 1, 1999

2. Interim report

3. "An Electrochemically-Driven Actuator Based on a Nanostructured Carbon Material"

4. GRANT: N00014-91J-1201, R&T CODE: 4133032

5. Guangli Che, Scott A. Miller, Ellen R. Fisher, and Charles R. Martin

6. Charles R. Martin, Department of Chemistry, Colorado State University, Fort Collins, CO 80523-1872

7. TECHNICAL REPORT NO. 31

8. Office of Naval Research, Chemistry Division, 800 North Quincy Street, Arlington, VA 22217-5660

9. To be published in *Analytical Chemistry*

10. Reproduction in whole or in part is permitted for any purpose of the United States Government. This document has been approved for public release and sale; its distribution is unlimited.

11. Abstract: A new type of electrochemically-driven actuator is described. This actuator uses graphitic carbon as the electroactive material (as opposed to the polymeric films used in previous devices of this type), and it is the first example of an actuator based on a nanostructured material. The actuator consists of branched carbon nanotubules embedded within the pores of a microporous alumina template membrane. Electrochemical Li^+ intercalation causes this nanotubule-containing membrane to flex, and electrochemical de-intercalation causes the membrane to relax to its original position. The characteristics of this new actuator are described here.

12. Subject terms: Artificial muscle, electrochemical actuator, carbon nanotubules

17. 18. 19. Unclassified

An Electrochemically-Driven Actuator Based on a Nanostructured Carbon Material

Guangli Che, Scott A. Miller, Ellen R. Fisher and Charles R. Martin*

Department of Chemistry,
Colorado State University,
Fort Collins, CO 80523.

*Corresponding Author, Email: crmartin@lamar.colostate.edu

Abstract

A new type of electrochemically-driven actuator is described. This actuator uses graphitic carbon as the electroactive material (as opposed to the polymeric films used in previous devices of this type), and it is the first example of an actuator based on a nanostructured material. The actuator consists of branched carbon nanotubules embedded within the pores of a microporous alumina template membrane. Electrochemical Li^+ intercalation causes this nanotubule-containing membrane to flex, and electrochemical de-intercalation causes the membrane to relax to its original position. The characteristics of this new actuator are described here.

INTRODUCTION

There has been considerable recent interest in electrochemically driven actuators, sometimes called "artificial muscles" [1-4]. Such actuators typically consist of a thin film of a polymeric material coated onto a flexible planar electrode surface. This assembly bends ("flexes") in response to an electrochemical perturbation of the polymeric material. The bent, flexed, state can then be returned to the straight, relaxed, state by reversal of the electrochemical perturbation. Electrochemically-driven actuators of this type based on the electronically conductive polymer polypyrrole have been extensively investigated [1-3]. In this case, the flexing/relaxing motion is driven by electrochemically oxidizing and reducing the polymer. More recently, Asaka et al. have described an actuator of this type based on the cationically-conductive polymer Nafion. A number of applications for such electrochemically-driven actuators have been suggested, including applications in robotics, single-cell capture and analysis, and microvalves that can be opened and closed upon electrochemical perturbation [1-3].

We have recently described a template-based [5] method for preparing carbon nanotubules [6]. This method entails using chemical vapor deposition (CVD) to deposit the carbon nanotubules within the pores of a microporous alumina membrane [6-8]. We have shown that these carbon nanotubules can electrochemically intercalate Li^+ and that this intercalation process is reversible. This prior work was done on carbon nanotubules of uniform diameter. We have

recently prepared membranes that contain carbon nanotubules that are highly branched at one end of the tubule.

We show here that electrochemical intercalation of Li^+ into these branched carbon-nanotubule membranes causes the membrane to flex and that the membrane can be returned to the relaxed state by simply electrochemically deintercalating the Li^+. It is the first actuator based on a nanostructured material. We have compared the response of this new carbon-based electrochemical actuator to analogous devices containing polypyrrole nanotubules. The carbon-based actuator showed superior flexing strength. This new nanostructured carbon actuator is described here.

EXPERIMENTAL

Materials. Ethylene (30% in helium), Li metal (Aldrich), and $FeCl_3$ (Aldrich) were used as received. Pyrrole (TCI 99%) was twice distilled under Ar. $LiClO_4$ (Aldrich) was dried at 150 °C for 24 hr under vacuum to remove water. Ethylene carbonate and diethyl carbonate (Aldrich) were distilled prior to use. The alumina template membranes used were Whatman Anodisc Filter Membranes (Fisher), designated as having 0.02 μm-diameter pores. In fact, these membranes contain 200 nm-dia. pores down most of their length, which branch into 20 nm-dia. pores (nominally) at one face of the membrane. Carbon nanotubule-membranes were also prepared from the straight-pore version (no branching) of this membrane. These membranes contain 200 nm-diameter pores. Both membranes are ~60 μm in thickness.

Preparation of the Carbon Nanotubule Membranes. Prior to CVD synthesis, the alumina template membranes were placed between two quartz plates, and this sandwich was heated at 900 °C for 30 min. in air. If this heat pretreatment is not done, the alumina membranes curl into a tight cylinder during the CVD synthesis (at 900 °C, *vide infra*) of C within the pores of the membrane. Heat pretreatment between quartz plates prevents this unwanted curling, and allows us to obtain planar C-containing membranes. This curling is associated with phase changes in the alumina from the initial hydrous oxide ultimately to gamma alumina. Because the surface area of the 20-nm pore-diameter face is so different from that of the 200-nm pore-diameter face, the volume change is different at the two faces causing curling of the membrane.

The CVD-based synthesis has been described previously [8]. Briefly, a 3.5 x 1.5 cm piece of the alumina template membrane was in the CVD reactor, and the reactor temperature was increased to 900 °C under argon flow. When the temperature stabilized the Ar flow was terminated, and simultaneously, a 10 sccm (standard cubic centimeter per min) flow of ethylene was initiated. Ethylene decomposes within the pores of the template membrane to yield the desired carbon nanotubules [8]. Carbon also deposits on both faces of the template membrane.

The amount of carbon deposited (i.e., the thickness of the walls of the carbon nanotubules and the surface layers) varies with the deposition time [8]. Unless otherwise noted, a deposition time of 30 min was used here. After

deposition, the Ar flow was resumed, the ethylene flow was terminated, and the furnace was turned off and allowed to cool to room temperature. The quantity of carbon deposited was determined gravimetrically by weighing the membrane before and after deposition.

Preparation of the Polypyrrole Nanotubule Membranes. These control membranes were prepared in order to compare the flexing strength of the carbon nanotubule membranes with that of an established artificial-muscle material [1-3]. The polypyrrole (PPy) tubules were deposited within the pores of the branched-pore alumina by oxidative polymerization of pyrrole [5]. A heat pretreated 3.5x1.5 cm piece of the alumina membrane was immersed into an aqueous 0.2 M pyrrole solution maintained at 5 °C. An equal volume of a 0.2 M $FeCl_3$ solution (also at 5 °C) was added and the oxidative polymerization was allowed to proceed for 4 hr. The membrane was then rinsed, dried in air, and the quantity of PPy deposited was determined gravimetrically.

Electrochemical Experiments. Electrochemical measurements were conducted with a computer-controlled EG&G PARC Model 263A potentiostat/galvanostat. A three-electrode cell, with either the carbon- or polypyrrole-nanotubule membrane as the working electrode and lithium foil as both the counter and reference electrodes, was used. The electrode configuration was as follows: The C-nanotubule-membrane working electrode was placed parallel to the rectangular Li-foil counter electrode, and the counter electrode had larger surface area than the nanotubule electrode. The branched-pore face of the

membrane faced the counter. The reference electrode was inserted into a Luggin capillary, and the tip was placed adjacent to the non-branched face of the C nanotubule working electrode. The electrolyte was 1 M $LiClO_4$ in a 30:70 (v/v%) mixture of ethylene carbonate and diethyl carbonate. All electrochemical experiments were conducted in a glove box filled with argon. The working electrodes were prepared by attaching a copper foil to the carbon surface layer covering the unbranched face of the membrane. Ag epoxy was used as the adhesive, and this epoxy was subsequently covered with nonconductive and inert Torr-Seal epoxy (Varian). The Ag epoxy and Cu foil covered less than 10% of the carbon nanotubule membrane surface. This insures that the flexing motion of the membrane is not inhibited by the Ag epoxy.

Electron Microscopy. Scanning electron microscopy (SEM) was used to image the surfaces of the carbon nanotubule membranes; a Phillips 505 microscope was used. The membrane was glued with the Torr-seal epoxy to an SEM sample holder, and 20 nm of Au-Pd was sputtered onto the surface using an Anatech sputter coater.

Transmission electron microscopy (TEM) was used to image the individual carbon nanotubules after removal from the alumina template membrane. A piece of the carbon/alumina membrane was immersed in concentrated HF overnight to dissolve the alumina. As discussed previously [6] this leaves a free-standing carbon nanotubule replica of the alumina membrane.

This carbon nanotubule membrane was removed from the HF and rinsed with water.

The membrane was then immersed into ethanol and sonicated for 20 min. This disrupts the carbon membrane and yields a suspension of the individual carbon nanotubules. A drop of this suspension was applied to a carbon-film coated TEM grid. The carbon nanotubules adhered well to this TEM grid and were easily imaged. TEM images were obtained using a JEOL 2000 microscope.

RESULTS AND DISCUSSION

Electron Microscopy. Figure 1 shows SEM images of the surfaces of the alumina template membrane after 30 min of CVD carbon deposition. In addition to forming the carbon nanotubules within the pores, both surfaces of the template membrane are coated with carbon films. The carbon surface film on the 200 nm pore-diameter face of the membrane is too thin to block the openings of the carbon nanotubules deposited within these pores (Figure 1A). However, because the pores on the branched-pore side of the membrane are so much smaller (nominally 20 nm) the carbon surface film completely covers this face of the membrane.

Both SEM and TEM were used to investigate the carbon nanostructures deposited within the ~20 nm-diameter pores beneath the carbon surface film that covers the branched-pore face of the membrane (Figure 1B). Figure 2A shows a cross-sectional SEM image of these carbon nanostructures after dissolution of

the alumina membrane; the branching of the nanostructures and the overlying C surface film, are clearly seen. Figure 2B shows a TEM image of three branched-pore C nanostructures, again after removal of the template membrane. The hollow 200 nm-diameter tubules that extend most of the length, as well as the branching at one end of the these tubules, are clearly seen. In addition, images of this type show that solid C nanofibers (as opposed to hollow nanotubules) are obtained at the branched-pore surface.

Figure 3 shows an electron diffraction pattern taken from a TEM sample like that shown in Figure 2. The brightest ring corresponds to the 002 reflection of hexagonal graphite. The intensity of this reflection is not, however, uniform across the ring, with two bright spots occurring at opposite positions across the ring (Figure 3). As discussed previously [8], this diffraction pattern indicates that the carbon is polycrystalline and that the carbon crystals have a preferred orientation within the nanotubules. Superimposing this diffraction pattern on the TEM image of the carbon nanotubule shows that the C*-axis is oriented perpendicular to the long axis of the tubule. The C*-axis in the graphite unit cell is perpendicular to the stacked layers [8]. Therefore, we can conclude that the graphitic layers have a preferential orientation parallel to the long axis of the nanotubule [8]. As will be discussed in the section on Mechanism, below, we believe that this preferred orientation plays a role in the electrochemically-induced "flexing" of this actuator.

Electrochemical Li^+ Intercalation. The electrochemical intercalation and de-intercalation reactions can be represented as follows [9]:

$$xLi^+ + xe^- + 6\ C \approx C_6Li_x \qquad (1)$$

X-ray photoelectron spectroscopy shows that after intercalation, the Li retains significant positive charge [10]; Correspondingly, the carbon atoms surrounding the Li^+ accumulate excess negative charge. The maximum value of x achieved in these experiments is 1.35.

Figure 4 shows a cyclic voltammogram associated with this reaction. The scan was started at the open circuit potential (3.0 V), well positive of the potential region where Li^+ is intercalated. As the potential is scanned negatively, a cathodic current is observed corresponding to the forward reaction in Equation 1 [6]. Upon scan reversal at 0 V, an anodic current is observed corresponding to the reverse reaction. At this low scan rate the anodic current ultimately decays to zero indicating complete removal of the intercalated Li^+. If the scan is interrupted, the current decays quickly to zero but the potential of the membrane does not change.

Performance of the Carbon-Nanotubule Membrane-Based Actuator. The vertical state of the membrane is the relaxed state, obtained at potentials near the open-circuit potential (~3 V vs. Li/Li^+). As the potential is scanned negatively, the membrane flexes in an upward direction toward the branched-

pore face. This flexing movement increases with decreasing potential during the voltammetric scan. The maximum flex, was obtained at an applied potential of ~0 V at the end of the forward voltammetric scan. Potentials negative of 0 V (vs. Li/Li^+) were not used because metallic Li is plated onto the membrane at such potentials. Upon scan reversal, the membrane relaxes back to the unflexed state.

The potential-dependent flexing movement was quantified in terms of the *horizontal* displacement of the tip of the C nanotubule membrane. A ruler was placed near the bottom of the electrochemical cell. The zero position of this ruler was aligned with the tip of the C nanotubule membrane when it was in its vertical, relaxed, state. The horizontal displacement of the tip was then measured relative to this zero position at various applied potentials during a cyclic voltammetric experiment.

The magnitude of the displacement, as defined in this way, depends on the length of the piece of carbon nanotubule membrane used. (The longer the strip of membrane, the greater the horizontal displacement.) This displacement could be normalized by dividing by the length of the membrane used (3.5 cm). Alternatively the angle that the flexed membrane makes with the vertical relaxed state might be used as a measure of the displacement. However, the flexed membrane is not straight, but rather is curved in an upward direction. This makes it difficult to define an angle of displacement.

Figure 5 shows the voltammetric current as a function of potential (A) and the corresponding potential-dependent displacement of the nanotubule membrane tip (B). The tip displacement increases continuously during the forward voltammetric scan and then relaxes back to the zero position during the reverse scan. These data make it clear that the flexing motion of this actuator is caused by electrochemical Li^+ intercalation. Figure 6 shows analogous data for three different voltammetric scan rates. Three points are worth making.

First, the extent of tip displacement decreases with increasing scan rate. This is because a smaller fraction of the carbon present becomes intercalated with Li^+ at higher scan rates (i.e., a smaller value of x in equation 1). Lower film utilization at higher sweep rates is a common phenomenon in thin-film cyclic voltammetry [10]. Briefly, at very low sweep rates, Li^+ diffusion in the carbon is sufficiently rapid that all of the carbon is utilized (Li^+-intercalated) during the voltammetric sweep. In contrast, at higher sweep rates, Li^+ diffusion is insufficiently rapid to intercalate all of the carbon, and Li^+ diffusion layers exist within carbon tubes and films (semi-infinite diffusion)[10]. Put another way, the carbon in the interior of the tubes and films is not utilized. As a result only a fraction of the carbon is utilized during the sweep [10].

Second, this lack of carbon utilization seems to be more pronounced for the de-intercalation process than for the intercalation process. Note that the anodic currents in Figure 6A are lower than the cathodic currents, and that the anodic current tails, a characteristic of semi-infinite diffusion [10]. This is reflected

in Figure 6B by the fact that, at high sweep rates, the membrane does not return to the totally relaxed state during the course of the voltammetric experiment. These data suggest (although certainly do not prove) that the apparent diffusion coefficient [10] associated with Li^+ intercalation into the carbon is higher than the apparent diffusion coefficient associated with the de-intercalation process. An alternative possibility is that the rates of electron transfer for the forward and reverse intercalation processes are different.

Third, the potential corresponding to the maximum displacement of the membrane tip always occurs when the current switches from cathodic to anodic (see downward arrows in Figure 6). This indicates that displacement continues as long as Li^+ intercalation is occurring (cathodic current), but stops when de-intercalation commences (onset of anodic current).

Figure 7 shows the effect of quantity of carbon deposited within the alumina template membrane on the displacement of this actuator. Quantity of carbon was varied by varying the duration of CVD-carbon synthesis. Figure 7 shows that actuator-movement increases with the quantity of carbon deposited.

Possible Response Mechanisms for this Actuator. Li^+-intercalation into graphite causes the spacing between the graphitic planes to increase from ~0.33 nm to ~0.37 nm [9] . Because the graphitic planes in these tubules are preferential oriented parallel to the tubule axes [8] , this lattice expansion must be accommodated by thickening of the tubules walls. This thickening processes will clearly exert a force against the alumina surrounding the tubule. However, at

the 200 nm-diameter C-tubule face of the membrane, this force can be partially dissipated because these tubules are hollow, allowing some room for expansion. That is, the force is partially dissipated by decreasing the inside diameter (as opposed to increasing the outside diameter) of these hollow tubules.

At the branched-pore face of the membrane, there are solid C nanofibers and much smaller inside-diameter C nanotubules (Figure 2B). As a result, there is little room for Intercalation-induced lattice expansion. This will cause the extent of Li^+ intercalation at the branched pore face of the membrane to be lower than at the open-pore face. We propose that it is this difference in extent of intercalation, and corresponding difference in potential across the thickness of the membrane that causes this electrochemical actuator to flex.

Comparison to an Analogous Polypyrrole-Based Actuator. Polypyrrole-based actuators or artificial muscles have been extensively investigated [1-3]. These devices typically consist of a polypyrrole film laminated onto a thin metal film to create a bilayer. In this case, flexing of the actuator is induced by electrochemically oxidizing the polypyrrole. This causes charge-balancing anions to be incorporated into the polymer, and in analogy to graphite, this results in an expansion of the polymeric material. However, the expansion in the case of polypyrrole is on the order of 1 to 3% [1-3], as opposed to ~12% for graphite [9].

In order to compare this new carbon–based actuator to a polypyrrole-based device, branched polypyrrole nanotubule membranes identical to the

carbon-nanotubule membranes discussed above were prepared. The mass of polypyrrole incorporated into these membranes was identical to the mass of C incorporated into the C nanotubule membranes (~10 mg) While these membranes showed cyclic voltammograms typical for polypyrrole [10], these membranes did not flex during the voltammetric scan. This is undoubtedly because of the lower expansion of polypyrrole, relative to carbon, and because polypyrrole is much more compressible than graphitic carbon.

CONCLUSIONS

A new type of electrochemically-driven actuator has been described. This actuator uses graphitic carbon as the electroactive material (as opposed to the polymeric films used in previous devices of this type), and it is the first example of a nanostructured actuator. A disadvantage of this actuator is that it requires non-aqueous solvents. However, the basic principle of this device – that a branched nanotubule causes intercalation-induced stress to be greater in the smaller branches than in the bigger "trunk" of the tubule – should be applicable to many different types of intercalation materials. Furthermore we have shown that the template method can used to prepare tubules of this type from many different types of materials [5]. We are currently searching for aqueous intercalation chemistry that utilizes a hard material; such chemistries and materials will be utilized in a second generation of nanostructured actuators of this type.

ACKNOWLEDGEMENTS. This work was supported by the Office of Naval Research and the Department of Energy.

References

1. Otero, T. F.; Rodriguez, J.; Santamora, C. Eur. *Pat.* **1992**, EP9200095.

2. Smela, E.; Inganas, O.; Lundstrom, I. *Science*, **1995**, *268*, 1735.

3. Pei, Q.; Inganas, O. *J. Phys. Chem.* **1992**, *96*, 10507.

4.Asaka, K.; Oguro, K.; Nishimara, Y.; Mizuhata, M.; Takenaka, H. *Polymer Journal,* **1995**, *27*, 436.

5. Martin, C. R., (a) *Science*, **1994**, *266,* 1961.; (b) *Acc. Chem. Res.*, **1995**, *8*, 1739.; (c) *Chem. Mater.*, **1996**, *8,* 1739.

6. Che, G.; Lakshmi, B. B.; Fisher, E. R.; Martin, C. R. *Langmuir* (in press).

7. Che, G.; Lakshmi, B. B.; Fisher, E. R.; Martin, C. R. *Nature*, **1998**, *393*, 346 .

8. Che, G.; Lakshmi, B. B.; Martin, C. R.; Fisher, E. R.; Ruoff, R. S., *Chem. Mater.* **1998**, *10,* 260.

9. Dahn, J. R.; Fong, R.; Spoon, M. J. *Phys. Rev. B*, **1990**, *42*, 6424.

10. Verbrugge, M. W.; Koch, B. J. *J.Electrrochem. Soc.* (a) **1996**, *143*, 24. (b) **1996**, *143*, 600.

10. Martin, C. R.; Rubinstein, I.; Bard, A. J. *J. Am. Chem. Soc.* **1982**, *104*, 4817.

Figure Captions

Figure 1. SEM images of the faces of the membrane after deposition of the carbon nanotubules and surface layers. A. 200 nm pore-diameter face of the membrane. B. Branched-pore face of the membrane.

Figure 2. A. SEM image of cross-section of carbon nanotubules after dissolution of the alumina membrane. B. TEM image of carbon nanotubules after dissolution of the alumina membrane.

Figure 3. Electron diffraction pattern obtained from a TEM sample like that shown in Figure 2.

Figure 4. Cyclic voltammogram associated with reversible Li^+ intercalation into the carbon-nanotubule-containing alumina membrane. Sweep rate = 0.1 mV/s.

Figure 5. A. Cyclic voltammogram plotted to more clearly show the cathodic (intercalation) and anodic (de-intercalation) scans. B. Distance the actuator moved during this voltammetric cycle. Sweep rate = 0.1 mV s^{-1}.

Figure 6. As per Figure 5 but at three different sweep rates . a. 0.1 mV s^{-1} , b. 0.8 mV s^{-1} , and c. 3 mV s^{-1} .

Figure 7. Actuator movement vs. quantity of carbon deposited into the alumina template membrane. Sweep rate = 0.1 mV s^{-1}.

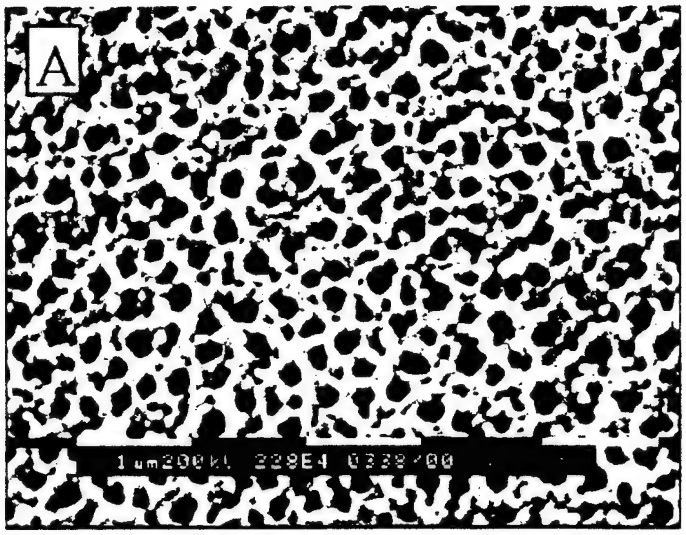

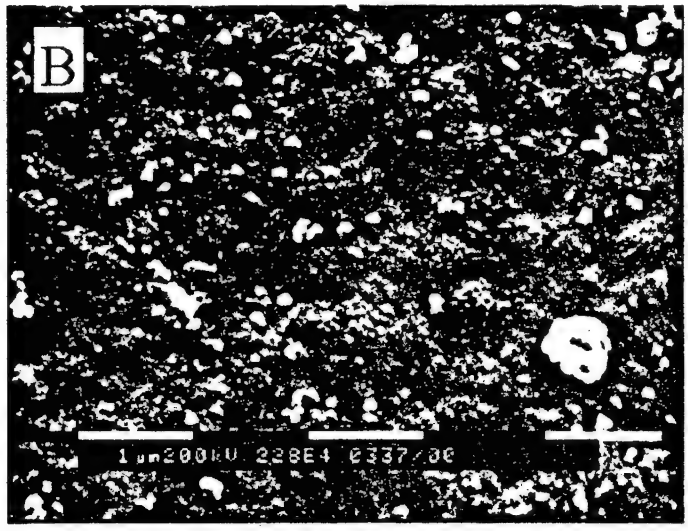

Fig 1

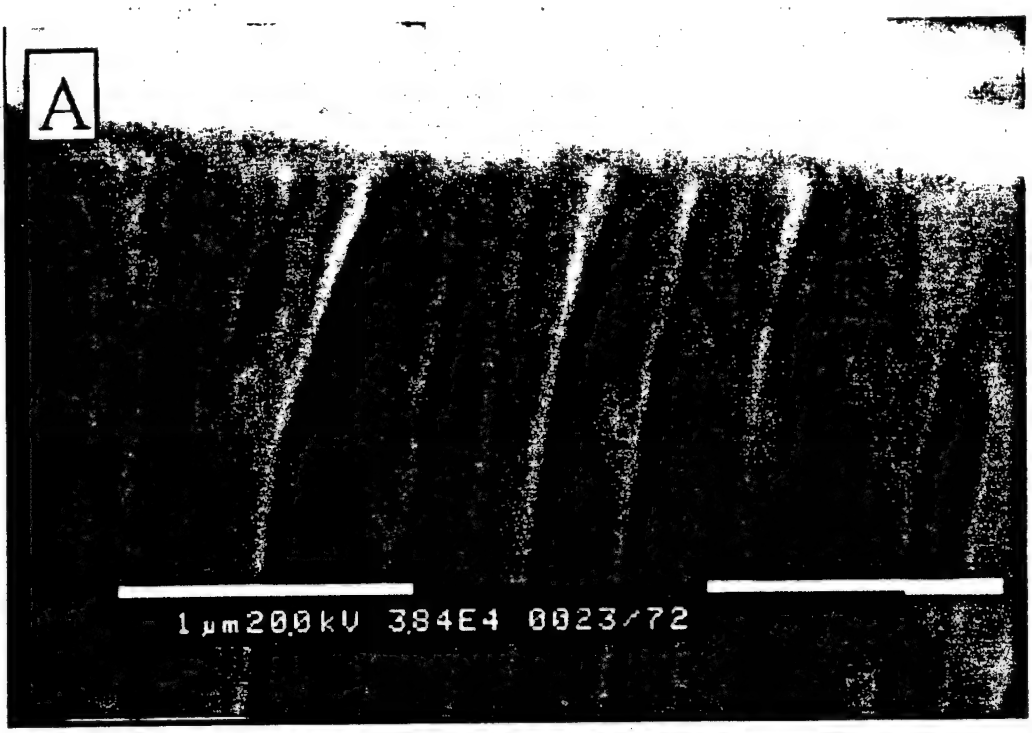

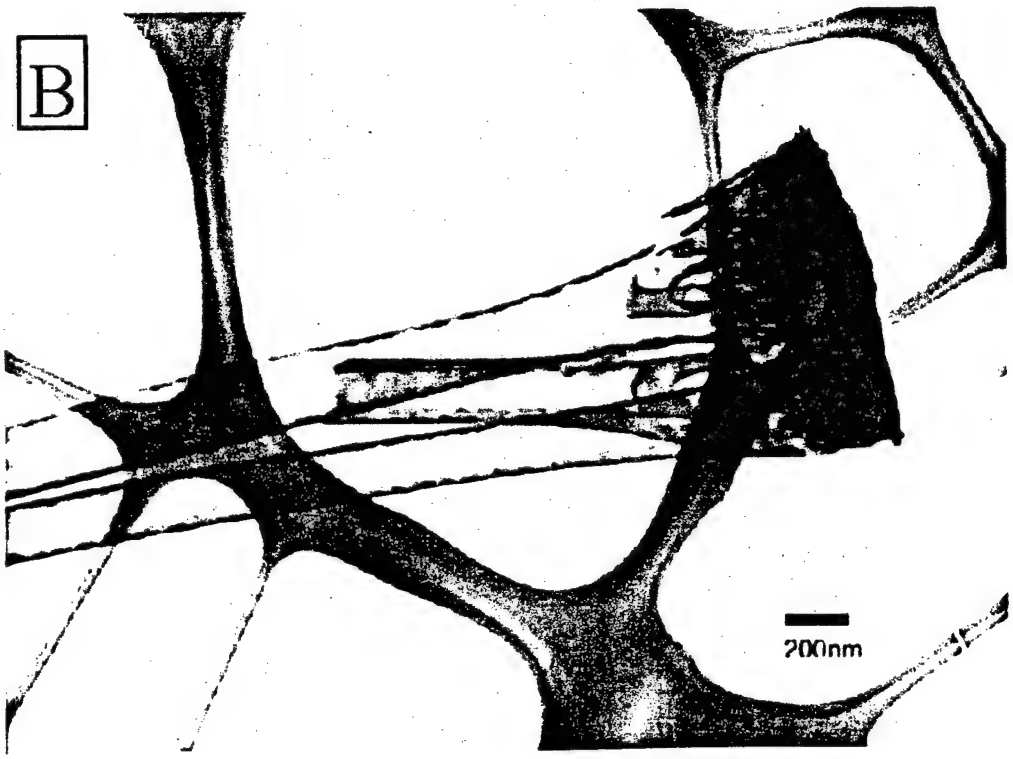

Fig. 2

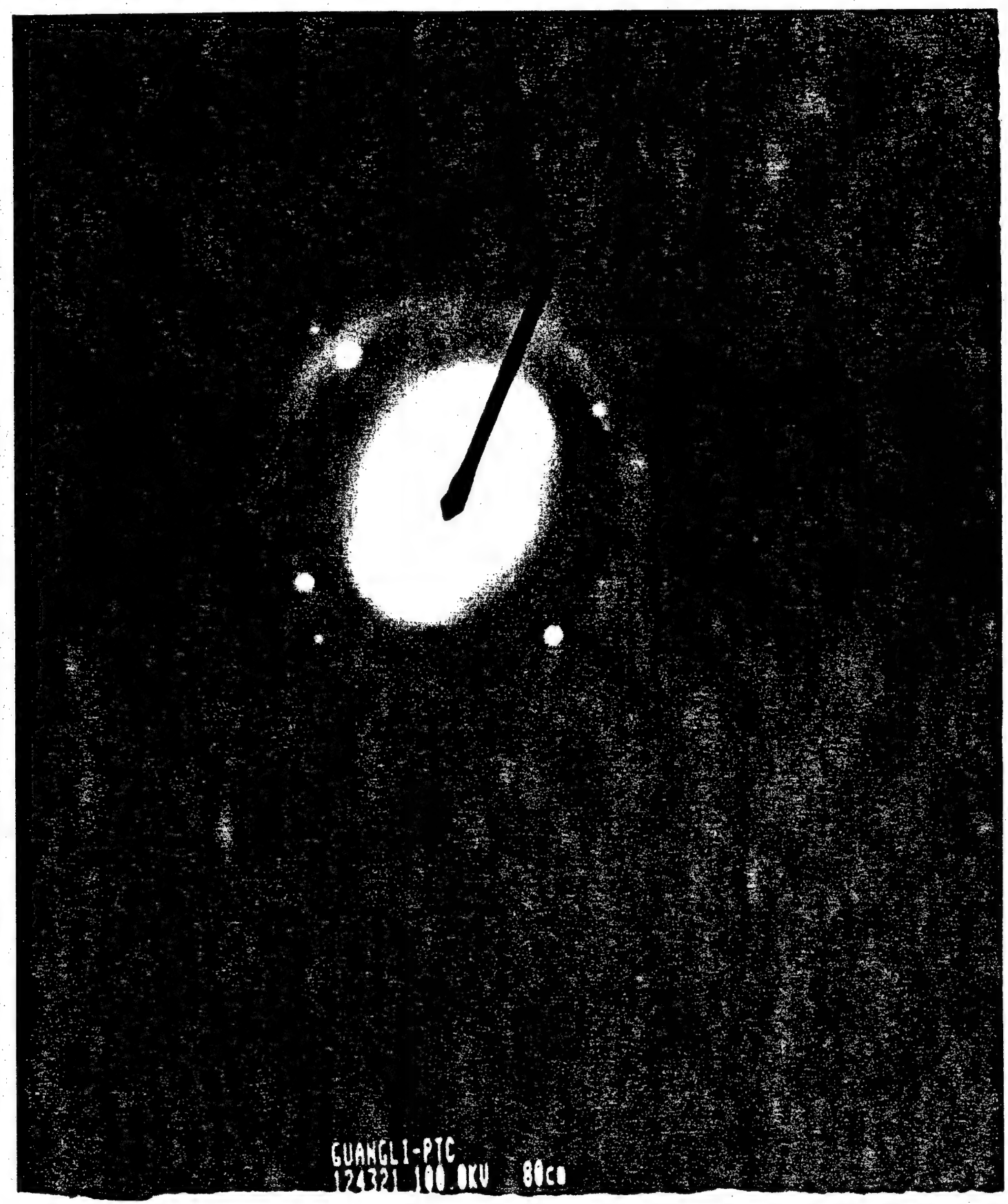

Fig.3

4

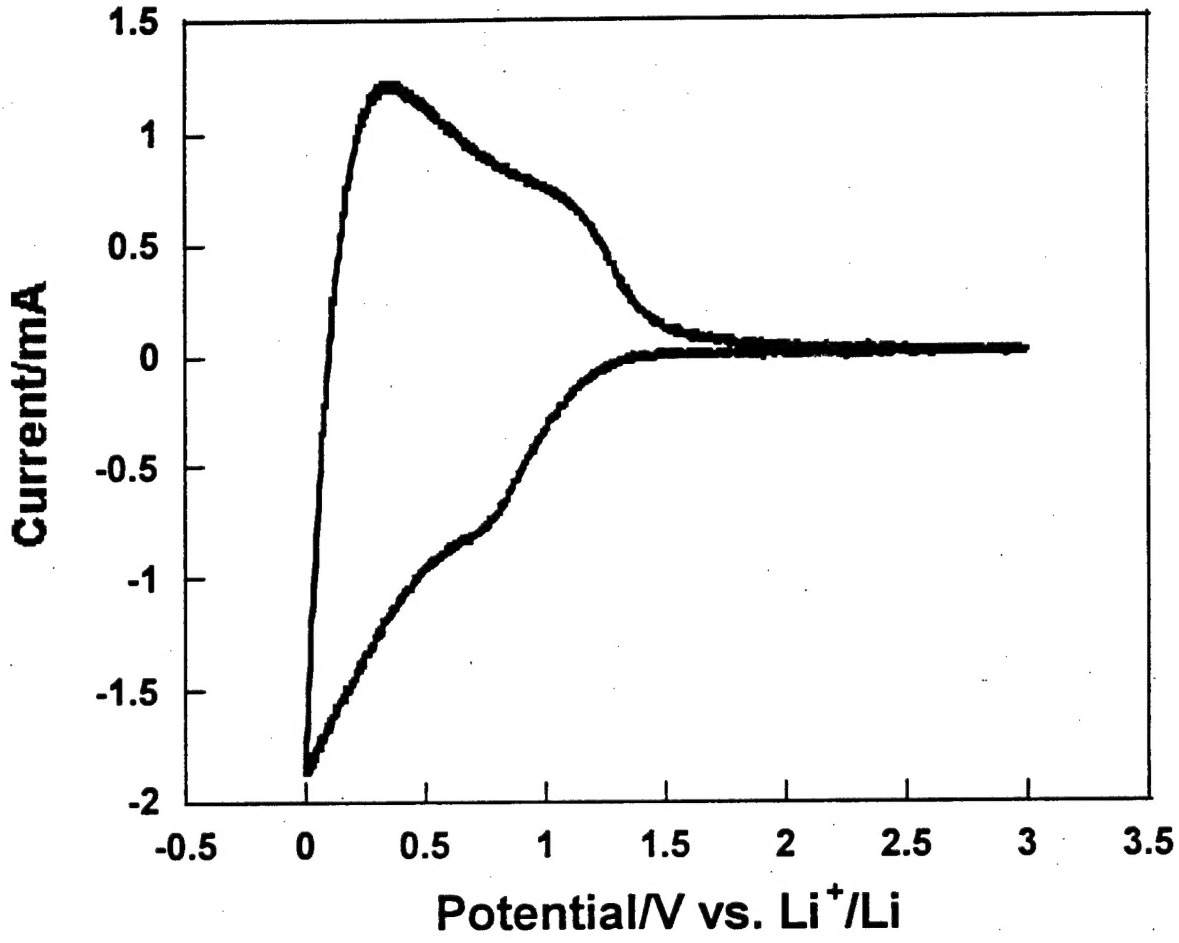
1.5
1
0.5
0
-0.5
-1
-1.5
-2
Current/mA
-0.5
0
0.5
1
1.5
2
2.5
3
3.5
Potential/V vs. Li+/Li

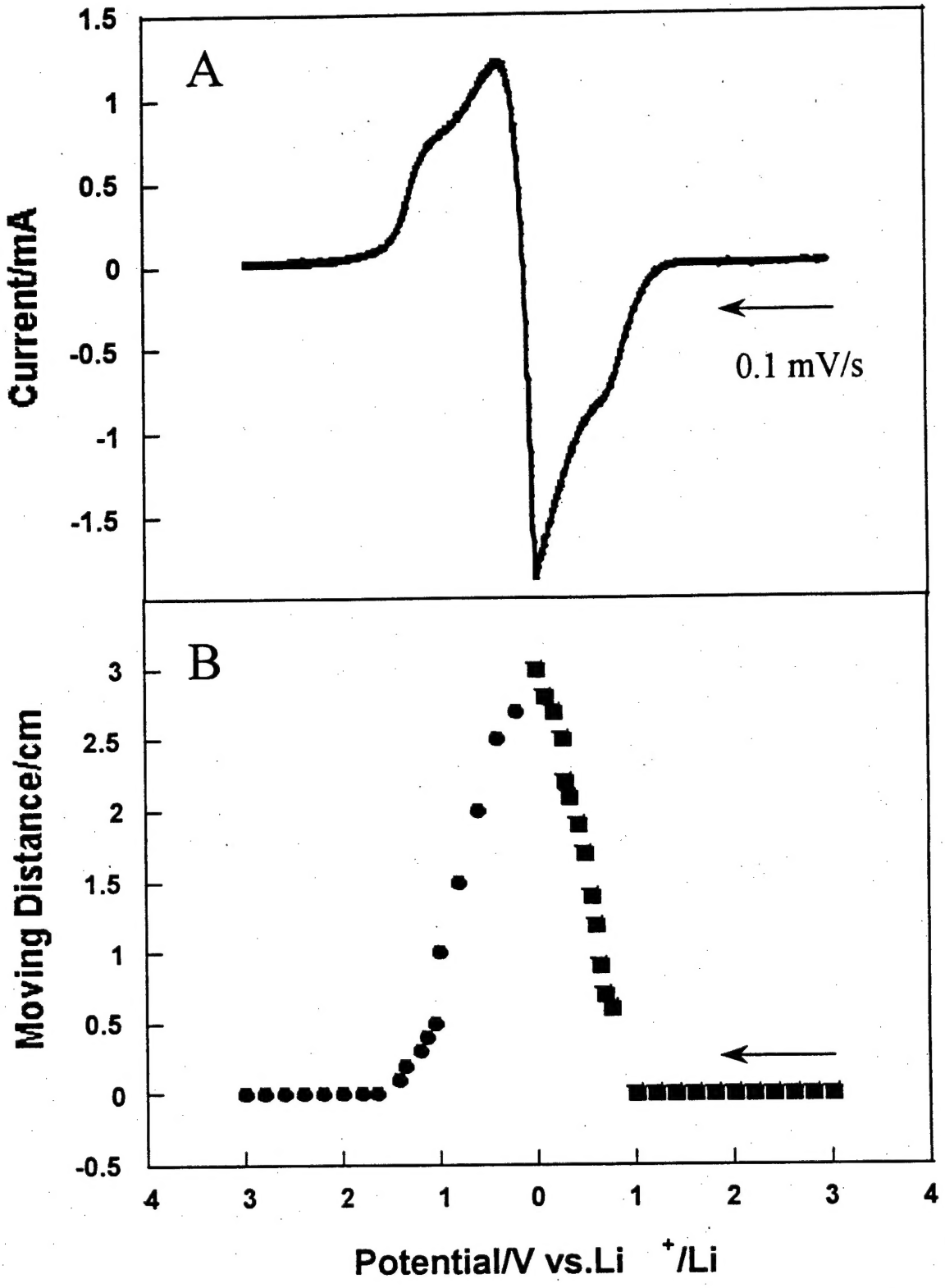
A
B
Current/mA
Moving Distance/cm
0.1 mV/s
1.5
1
0.5
0
-0.5
-1
-1.5
3
2.5
2
1.5
1
0.5
0
-0.5
4
3
2
1
0
1
2
3
4
Potential/V vs.Li +/Li

6

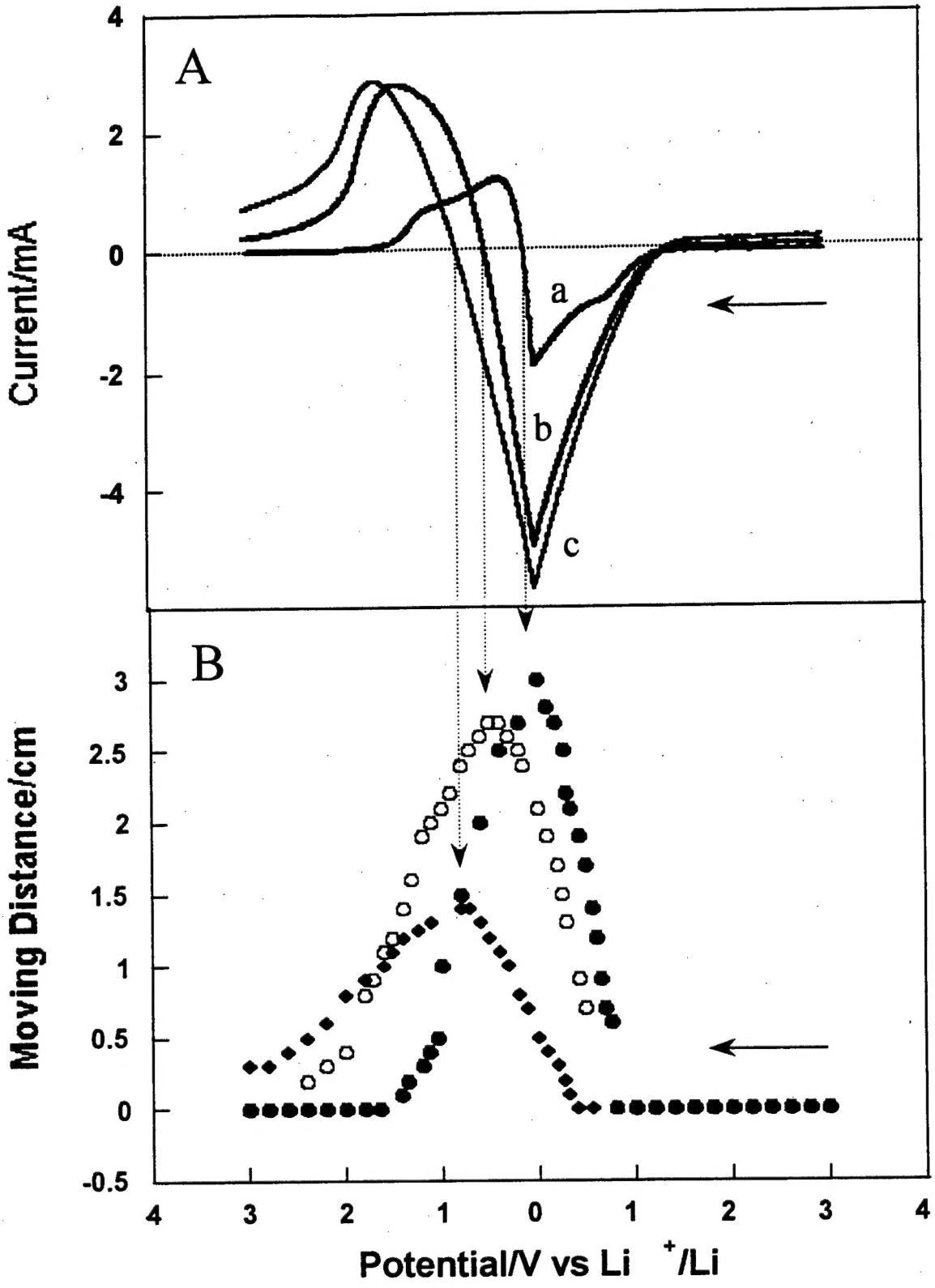
A
B
a
b
c
Current/mA
Moving Distance/cm
Potential/V vs Li +/Li
4
2
0
-2
-4
3
2.5
2
1.5
1
0.5
0
-0.5
4
3
2
1
0
1
2
3
4

7

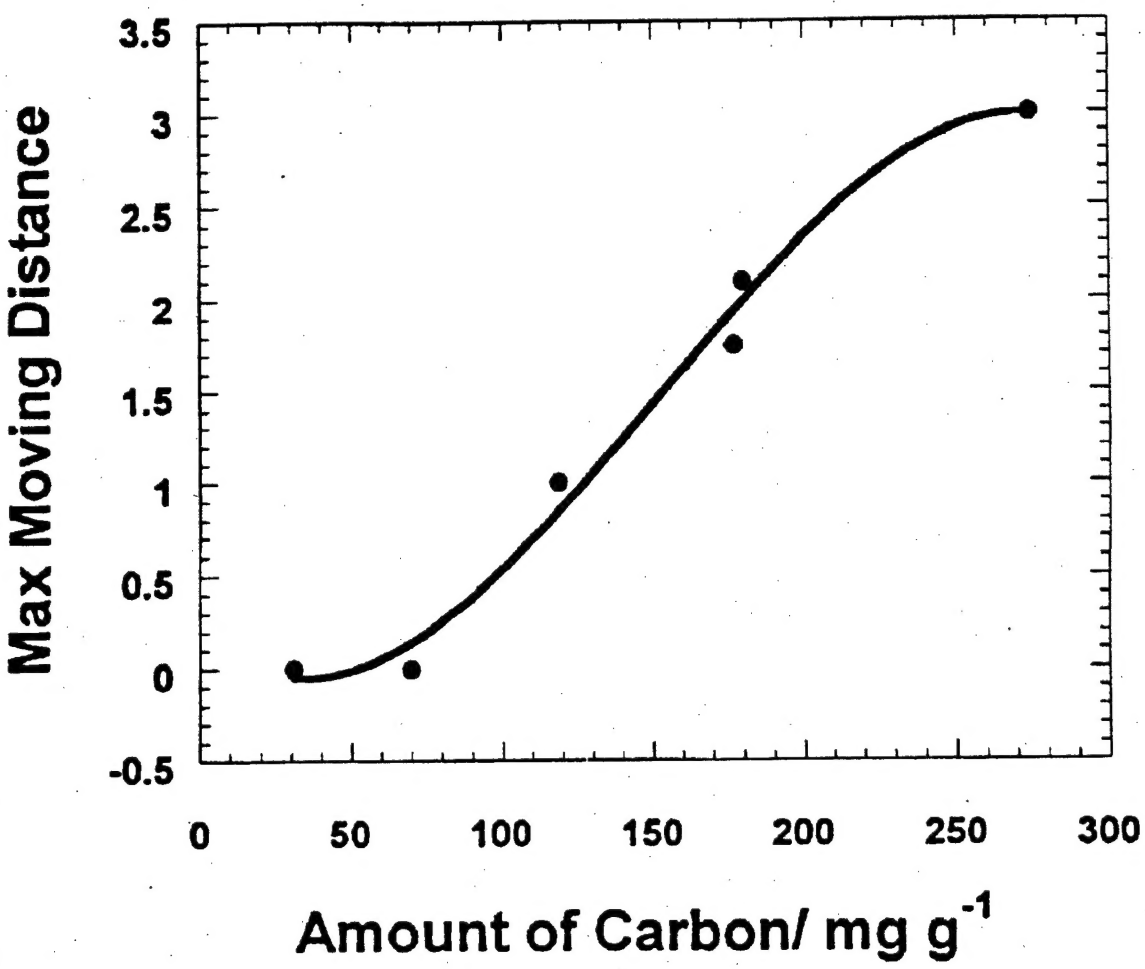
Max Moving Distance
3.5
3
2.5
2
1.5
1
0.5
0
-0.5
0
50
100
150
200
250
300
Amount of Carbon/ mg g-1